

Particle-Particle Particle-Tree: A Direct-Tree Hybrid Scheme for Collisional N -Body Simulations

Shoichi OSHINO^{1,2}, Yoko FUNATO⁴, and Junichiro MAKINO^{1,2,3}

¹*Department of Astronomical Science, The Graduate University for Advanced Studies (SOKENDAI),
2-21-1 Osawa, Mitaka, Tokyo 181-8588*

²*Division of Theoretical Astronomy, National Astronomical Observatory of Japan, 2-21-1 Osawa,
Mitaka, Tokyo 181-8588*

oshino@cfca.jp

³*Center for Computational Astrophysics, National Astronomical Observatory of Japan, 2-21-1
Osawa, Mitaka, Tokyo 181-8588*

makino@cfca.jp

⁴*Department of General System Studies, Graduate School of Arts and Sciences, The University of
Tokyo, 3-8-1 Komaba, Meguro, Tokyo 153-8902*

funato@artcompsci.org

(Received 2011 January 19; accepted)

Abstract

In this paper, we present a new hybrid algorithm for the time integration of collisional N -body systems. In this algorithm, gravitational force between two particles is divided into short-range and long-range terms, using a distance-dependent cutoff function. The long-range interaction is calculated using the tree algorithm and integrated with the constant-timestep leapfrog integrator. The short-range term is calculated directly and integrated with the high-order Hermite scheme. We can reduce the calculation cost per orbital period from $O(N^2)$ to $O(N \log N)$, without significantly increasing the long-term integration error. The results of our test simulations show that close encounters are integrated accurately. Long-term errors of the total energy shows random-walk behaviour, because it is dominated by the error caused by tree approximation.

Key words: methods: n-body simulations — solar system: formation

1. Introduction

For the time integration of collisional N -body systems such as star clusters and systems of planetesimals, the combination of direct summation for force calculation and the individ-

ual timestep algorithm has been the standard method for nearly half century (Aarseth 1963, 2003). For galactic dynamics and cosmology, fast and approximate methods for force calculation such as the particle-mesh scheme (Hockney & Eastwood 1981), the P³M scheme (Hockney & Eastwood 1981), the tree method (Barnes & Hut 1986) and combinations of PM and tree (Xu 1995, Bagla 2002, Dubinski et al. 2004, Springel 2005, Yoshikawa & Fukushige 2005, Ishiyama et al. 2009) are used. It is not impossible to combine individual timestep algorithm and fast and approximate force calculation. For example, McMillan & Aarseth (1993) developed a high-order integrator using individual timestep combined with the tree algorithm. However, it was difficult to achieve good performance on distributed-memory parallel computers for such scheme. Fujii et al. (2007) introduced a hybrid of tree and individual timestep algorithm, which is designed to handle the evolution of star clusters embedded in the parent galaxy. In their BRIDGE scheme, both the parent galaxy and the star cluster are expressed as N -body systems. The interaction between particles in the star cluster are calculated directly and integrated with the individual timestep scheme, while interactions between particles in the parent galaxy and that between particles in parent galaxy and particles in star clusters are calculated with the tree algorithm and integrated with the leapfrog scheme with shared and constant timesteps.

The BRIDGE scheme is based on the idea of splitting the Hamiltonian of an N -body system to multiple components. The time integration of tree part is symplectic and does not generate any secular error. The direct integration of the internal motion of star cluster is not symplectic, but treated with high accuracy using high-order integrators. The obvious limitation of the BRIDGE scheme is that it can handle the close encounters of particles in star clusters only. If we want to allow close encounter between particles in the parent galaxy, it goes back to the usual direct summation scheme.

For the time integration of planetary systems, the mixed variable symplectic (hereafter MVS) scheme (Kinoshita, Yoshida & Nakai 1991, Wisdom & Holman 1991) has become the standard method. For the time integration of almost stable orbits of planets, the MVS is well suited. However, if we want to handle protoplanets or planetesimals, we need to handle their close encounters and collisions. The MVS scheme, however, cannot handle them since it requires that the timestep is kept constant (Calvo & Sanz-Serna 1993). In order to handle close encounters, several modifications of MVS method have been proposed. One is the hybrid method by Chambers (1999). It handles close encounters with high accuracy by splitting the Hamiltonian to that of close interaction and distant interaction as in the case of P³M method. It can be used for planetary accretion problems. However, it relies on the direct calculation and its calculation cost scales as $O(N^2)$. Very recently, Moore, Quillen & Edgar (2008) applied GPGPU to the hybrid method. In addition, they used the Hermite scheme (Makino & Aarseth 1992) for the integration of the short range force.

Brunini & Viturro (2003) and Brunini et al. (2007) combined the hybrid method and the tree algorithm. Therefore their method can handle a large number of particles and close

encounters. The scheme described in Brunini & Viturro (2003) uses the leapfrog integrator to handle the Hamiltonian for the short-range interaction. Therefore it had to use very small timesteps. The scheme described in Brunini et al. (2007) seems to be improved, but no details of the scheme was given.

In this paper, we describe a new time integration algorithm which combines the strong points of these schemes. This scheme is combination of the BRIDGE scheme (Fujii et al. 2007) and a hybrid symplectic integrator method (Chambers 1999). We call this scheme as Particle-Particle Particle-Tree (hereafter PPPT). In section 2 we overview previous numerical methods. These methods are based on the MVS method. Therefore, we first introduce the MVS method and then overview extension of MVS method. In section 3 we describe our new time integration algorithm, PPPT. In section 4, we show the result of test simulations. In this paper, we discuss only the simulations of planet formation process. However, in future works, we apply PPPT to other collisional systems. Summary and discussions are given in section 5.

2. The Numerical Method

2.1. The symplectic integrator

The Hamiltonian of an N -body system is given by

$$H = \sum_i^N \frac{p_i^2}{2m_i} - \sum_{i=1}^{N-1} \sum_{j=i+1}^N \frac{Gm_i m_j}{r_{ij}}, \quad (1)$$

where p_i is the momentum of particle i , r_{ij} is the distance between particles i and j , m_i is the mass of particle i and G is the gravitational constant. The Hamilton's equation of motion is

$$\frac{df}{dt} = \{f, H\}, \quad (2)$$

where $\{f, H\}$ is the Poisson bracket and f is a canonical variable. We define the differential operator as $Df \equiv \{f, H\}$. The general solution of equation (2) at time $t + \Delta t$ is formally written as

$$f(t + \Delta t) = e^{\Delta t D} f(t). \quad (3)$$

Equation (3) cannot be solved analytically. We can obtain the approximate solution by dividing the Hamiltonian into multiple parts that can be analytically solved.

In the symplectic integrator, the Hamiltonian is divided into two parts as

$$H = H_A + H_B, \quad (4)$$

$$H_A = - \sum_{i=1}^{N-1} \sum_{j=i+1}^N \frac{Gm_i m_j}{r_{ij}}, \quad (5)$$

$$H_B = \sum_i^N \frac{p_i^2}{2m_i}, \quad (6)$$

where H_A is the potential energy and H_B is the kinetic energy, and each of which can be solved.

The time evolution of f is given by

$$f(t + \Delta t) = e^{\Delta t D} f(t) = e^{\Delta t(A+B)} f(t), \quad (7)$$

where $A \equiv \{, H_A\}$ and $B \equiv \{, H_B\}$ are operators. The exponential in equation (7) can be approximated as

$$e^{\Delta t(A+B)} = \prod_{i=1}^k e^{a_i \Delta t A} e^{b_i \Delta t B} + O(\Delta t^{n+1}), \quad (8)$$

where (a_1, a_2, \dots, a_k) and (b_1, b_2, \dots, b_k) are real numbers, k is the number of stages, n is the order of approximation. The first term of the right hand side of equation (8) is an order- n approximation of the left hand side. The first-order symplectic integrator is given by

$$f(t + \Delta t) = e^{\Delta t A} e^{\Delta t B} f(t) + O(\Delta t^2), \quad (9)$$

and the second-order symplectic integrator, which is the leapfrog integrator, is given by

$$f(t + \Delta t) = e^{\Delta t A/2} e^{\Delta t B} e^{\Delta t A/2} f(t) + O(\Delta t^3). \quad (10)$$

The symplectic integrator has the advantage that there is no long-term energy error for the time integration of periodic systems. In the case of a near-Kepler potential, both the semi-major axis and the eccentricity are conserved. One disadvantage of the symplectic method is that high-order schemes are expensive and have rather large local error coefficients. Another disadvantage is that it requires a constant timestep. If we change the timestep following usual recipes for Runge-Kutta-Fehlberg-type schemes (Fehlberg 1968), the energy is no longer conserved (Skeel & Gear 1992, Calvo & Sanz-Serna 1993). There are a number of proposals for methods to combine the variable timesteps and the good nature of the symplectic schemes. Most of them are based on the idea of splitting the potential to fast-varying and second-varying terms and applying different timesteps. For example, Skeel & Biesiadecki (1994) proposed a method that splits the gravitational force into many components, each of which has finite effective range in the distance. By assigning different timesteps to different components, they effectively realized a variable timestep integration.

The methods discussed below are all based on the idea of changing the way to split the Hamiltonian.

2.2. The Mixed Variable Symplectic Method

Kinoshita, Yoshida & Nakai (1991) and then Wisdom & Holman (1991) introduced the MVS method for planetary systems. In the symplectic scheme, we split the Hamiltonian to kinetic and potential energy, so that we have analytical solutions for both parts. This division is not unique. As far as each splitted Hamiltonian has an analytic solution, any division can be used. The idea of MVS is to split the Hamiltonian to the Keplerian term H_{Kep} and interaction term H_{Int} . The time evolution is given by

$$H = H_{Kep} + H_{Int}, \quad (11)$$

$$f(t + \Delta t) = e^{\Delta t K/2} e^{\Delta t I} e^{\Delta t K/2} f(t), \quad (12)$$

where K is the operator defined as $Kf \equiv \{f, H_{Kep}\}$ and I is the operator defined as $If \equiv \{f, H_{Int}\}$. The MVS method integrates H_{Int} with the leapfrog integrator and H_{Kep} by using analytic solution of the Kepler orbit. Thus the MVS method is expressed as follows:

1. Calculate accelerations due to gravitational interactions between planets at time t and give a velocity kick.
2. Update analytically positions and velocities from t to $t + \Delta t$ by using the Solar gravity.
3. Calculate accelerations due to gravitational interactions between planets at time $t + \Delta t$ and give a velocity kick.

The advantage of MVS is that only interactions between planets are integrated numerically. The Solar gravity is analytically integrated and is accurate up to the round-off error.

2.3. The BRIDGE code

The BRIDGE code was introduced by Fujii et al. (2007). It was designed for the time integration of star clusters embedded in parent galaxies. This scheme is a combination of the direct and a tree schemes, using the idea similar to that of the MVS scheme. The internal interactions of stars in star clusters are integrated by the Hermite integrator with direct summation, while other parts are integrated by the leapfrog integrator and tree scheme.

The BRIDGE scheme divides the Hamiltonian as

$$H = H_\alpha + H_\beta, \quad (13)$$

$$H_\alpha = - \sum_{i < j}^{N_G} \frac{G m_{G,i} m_{G,j}}{r_{GG,ij}} - \sum_{i=1}^{N_G} \sum_{j=1}^{N_{SC}} \frac{G m_{G,i} m_{C,j}}{r_{GC,ij}}, \quad (14)$$

$$H_\beta = \sum_{i=1}^{N_G} \frac{p_{G,i}^2}{2m_{G,i}} + \sum_{i=1}^{N_{SC}} \frac{p_{C,i}^2}{2m_{C,i}} - \sum_{i < j}^{N_{SC}} \frac{G m_{C,i} m_{C,j}}{r_{CC,ij}}, \quad (15)$$

where N_G and N_{SC} are the number of particles in the parent galaxy and that in the star cluster, $m_{G,i}$ and $p_{G,i}$ are the mass and the momentum of particle i in the galaxy, $m_{C,i}$ and $p_{C,i}$ are those of particle i in the star cluster, and r_{GG}, r_{GC}, r_{CC} are distances between two galaxy particles, one galaxy and one star cluster particle, and two star cluster particles, respectively. We can express the time evolution from t to $t + \Delta t$ as

$$f(t + \Delta t) = e^{\frac{1}{2}\Delta t \alpha} e^{\Delta t \beta} e^{\frac{1}{2}\Delta t \alpha} f(t), \quad (16)$$

where α is the operator defined as $\alpha f \equiv \{f, H_\alpha\}$ and β is the operator defined as $\beta f \equiv \{f, H_\beta\}$.

The BRIDGE code uses the leapfrog scheme for H_α , and the fourth-order Hermite scheme for H_β . Thus the integration procedure during a tree timestep Δt is done in the following way:

1. Make a tree at time t and calculate accelerations from all particles on galaxy particles, and from galaxy particles on star-cluster particles.
2. Give a velocity kick for star cluster particles, and update the velocities of galaxy particles.

3. Integrate positions and velocities of star cluster particles from t to $t + \Delta t$ by using the Hermite scheme with the individual timestep, and positions of galaxy particles by making them drift with the constant velocities.
4. Make a new tree at $t + \Delta t$ and calculate accelerations from all particles to galaxy particles, and from galaxy particles to star cluster particles.
5. Give a velocity kick for star cluster particles and update velocities for galaxy particles.

In this scheme, H_α is integrated with the symplectic leapfrog scheme, while H_β is integrated with non-symplectic Hermite scheme. It combines the fast tree code for the orbital motion of particles in the galaxy and high-accuracy Hermite scheme for the internal orbital motion of particles in the star cluster without any additional approximation. Thus, it is the first scheme with which we can follow the orbital and internal evolution of a star cluster embedded in a galaxy in a fully self-consistent way.

2.4. The MERCURY code

The MERCURY code (Chambers 1999) splits the Hamiltonian into three parts as

$$H = H_{Kep} + H_{Int} + H_{Sun}, \quad (17)$$

$$H_{Kep} = \sum_{i=1}^N \left(\frac{p_i^2}{2m_i} - \frac{Gm_i m_\odot}{r_i} \right) - \sum_{i<j}^N \frac{Gm_i m_j}{r_{ij}} W(r_{ij}), \quad (18)$$

$$H_{Int} = - \sum_{i<j}^N \frac{Gm_i m_j}{r_{ij}} (1 - W(r_{ij})), \quad (19)$$

$$H_{Sun} = \sum_{i=1}^N \frac{p_i^2}{2m_\odot}, \quad (20)$$

where H_{Int} is the potential energy of gravitational interactions between particles except for those undergoing close encounters, H_{Kep} is the kinetic energy of particles plus potential energy of particles undergoing close encounters, H_{Sun} is the kinetic energy of the Sun, and $W(r_{ij})$ is the changeover function. The modification from MVS is that the potential energy of nearby particles is separated from H_{Int} and moved to H_{Kep} . The time evolution is described as

$$f(t + \Delta t) = e^{\frac{1}{2}\Delta t I} e^{\frac{1}{2}\Delta t S} e^{\Delta t K} e^{\frac{1}{2}\Delta t S} e^{\frac{1}{2}\Delta t I} f(t). \quad (21)$$

where I is the operator defined as $I f \equiv \{f, H_I\}$, S is the operator defined as $S f \equiv \{f, H_S\}$ and K is the operator defined as $K f \equiv \{f, H_K\}$. This scheme is sometimes called the hybrid scheme. In the actual code (MERCURY), the force from gravitational interactions is split instead of the Hamiltonian for the ease of programming. We can write the pairwise force $F(r_{ij})$ as

$$F(r_{ij}) = F_{close}(r_{ij}) + F_{dist}(r_{ij}), \quad (22)$$

$$F_{close}(r_{ij}) = F(r_{ij})K(r_{ij}), \quad (23)$$

$$F_{dist}(r_{ij}) = F(r_{ij})[1 - K(r_{ij})], \quad (24)$$

where $F_{close}(r_{ij})$ is the force for close encounter and $F_{dist}(r_{ij})$ is the remaining force. The relation between W and K is given by

$$W(r) = r \int_r^\infty \frac{K(x)}{x^2} dx \quad (25)$$

In the hybrid scheme, H_{Kep} does not have an analytical solution if the potential of close encounter is not zero. Therefore, Kf is integrated numerically using the Bulirsch-Stoer method (Bulirsch & Stoer 1964 and Stoer & Bulirsch 1980). The one-step integration of the hybrid scheme is done in the following way:

1. Apply the velocity kick, $e^{\Delta\frac{1}{2}tI}$, due to distant interaction H_{Int} .
2. Apply the position drift $e^{\Delta\frac{1}{2}tS}$, due to H_{Sun} .
3. Integrate orbits of particles which are under close encounters using BS method, and update positions and velocities of the rest of particles using the Kepler orbit.
4. Give the position drift by H_{Sun} with stepsize $\Delta t/2$.
5. Give the velocity kick by H_{Int} with stepsize $\Delta t/2$.

The hybrid method is used for long-term integrations of outer solar system, restricted three-body problems, and planetary embryos. It has a good performance for accuracy and speed for small- N systems, but for system with a large number of particles it becomes expensive.

2.5. The DAEDALUS code

Brunini et al. (2007) presented a new mixed-variables symplectic tree code for planetesimal dynamics, DAEDALUS. This code is an improved version of the modified tree code described in Brunini & Viturro (2003). Brunini & Viturro (2003) developed the tree code (Barnes & Hut 1986) with two-level timesteps for planetesimal systems. This tree code usually integrates all particles with a constant timestep using the leapfrog integrator. If close encounters occur, it integrates only particles which undergo close encounters with much smaller timesteps. When integrating close encounters, timesteps are determined using equation (2) in Brunini & Viturro (2003), and the tree is constructed at each steps.

The DAEDALUS integrator is combination of the tree code and a hybrid symplectic integrator method. It splits the Hamiltonian following the description of Chambers (1999). Therefore the DAEDALUS integrator integrates H_{Int} using tree method and integrates H_{Kep} analytically where there are no close encounters. If close encounters occur, it integrates H_{Kep} numerically using the Bulirsch-Stoer method. The one-step integration of the DAEDALUS integrator is done in the following way:

1. Make a tree and calculate accelerations from H_{Int} then give a velocity kick.
2. Give a position drift by H_{Sun} with stepsize $\Delta t/2$.
3. Calculate positions and velocities for particles which are in close encounters, and update positions and velocities with the Kepler orbit for particles which are not in close encounters.
4. Apply the position drift $e^{\Delta\frac{1}{2}tS}$, due to H_{Sun} .

	Tree method	distant-based criterion	variable timestep	individual timestep
MVS	-	-	-	-
MERCURY	-	○	○	-
BRIDGE	○	-	○	○
DAEDALUS	○	○	○	-
This paper	○	○	○	○

Table 1. Characteristics of each method.

5. Make a new tree at next step and calculate accelerations from H_{Int} then give a velocity kick.

The DAEDALUS integrator uses the variable, but shared, timestep for close encounters. Therefore, when the number of particles in close encounters is large, the calculation cost can become high. If we use an individual timestep, we can decrease the calculation cost significantly. In Table 1, we summarize the characteristics of the previous and present algorithms. Table 1 shows that there were no algorithms which has all of the listed desirable properties except for the one described in this paper. In this paper, we present a new algorithm which uses the shared timestep for distant interactions and the individual timestep for close interactions. Furthermore, the force due to distant interactions are calculated by using tree method with a changeover function.

3. Particle-Particle Particle-Tree (PPPT) scheme

In this section we describe our new scheme for collisional N -body systems. We use the fourth-order Hermite method for near-neighbour forces and the tree method for distant forces, and we use the hybrid method to split the gravitational force by using a changeover function. In our scheme, we split the gravitational force between two particles as

$$F(r_{ij}) = F_{Hard}(r_{ij}) + F_{Soft}(r_{ij}), \quad (26)$$

$$F_{Hard}(r_{ij}) = F(r_{ij})K(r_{ij}), \quad (27)$$

$$F_{Soft}(r_{ij}) = F(r_{ij})[1 - K(r_{ij})], \quad (28)$$

where $F_{Hard}(r_{ij})$ is the force from nearby particles and $F_{Soft}(r_{ij})$ is the force from distant particles. These formulae are the same as equations (22)-(24). We can write the Hamiltonian as

$$H = H_{Hard} + H_{Soft}, \quad (29)$$

$$H_{Hard} = \sum_{i=1}^N \left(\frac{p_i^2}{2m_i} - \frac{Gm_i m_\odot}{r_i} \right) - \sum_{i<j}^N \frac{Gm_i m_j}{r_{ij}} W(r_{ij}), \quad (30)$$

$$H_{Soft} = \sum_{i<j}^N \frac{Gm_i m_j}{r_{ij}} (1 - W(r_{ij})), \quad (31)$$

where H_{Hard} contains the kinetic energy of all particles and the potential energy of near-neighbours, and H_{Soft} contains the potential energy of all other pairs of particles. We treat the solar gravity as the force caused by a fixed potential in this paper. So we do not have H_{Sun} here. We can express the time evolution from t to $t + \Delta t$ as

$$f(t + \Delta t) = e^{\frac{1}{2}\Delta t S} e^{\Delta t H} e^{\frac{1}{2}\Delta t S} f(t). \quad (32)$$

The changeover function K splits the gravitational force between particles to contributions of close encounters and others. Thus, H_{Hard} changes rapidly and H_{Soft} changes slowly. In this paper, we use two types of changeover functions. One is the fourth order spline function which introduced by Abe et al. (1986) given as

$$K(r_{ij}) = \left(\frac{\sin X}{X} \right)^5, \quad (33)$$

where $X = \pi r_{ij}/r_{cut}$ and r_{cut} is a scaling radius. Note that $K(r_{ij})$ becomes zero where $r_{ij} \geq r_{cut}$ (see fig 1). The other was first introduced by Levison & Duncan (2000). It is given by

$$K(r_{ij}) = \begin{cases} 1 & \text{if } Y \geq 1, \\ 10Y^6 - 15Y^8 + 6Y^{10} & \text{if } 0 < Y < 1, \\ 0 & \text{if } Y \leq 0, \end{cases} \quad (34)$$

where $Y = \frac{r_2 - r_{ij}}{r_2 - r_1}$. Hereafter we call it the DLL function. In figure 1, $r_1/r_{cut} = 0.4$ and $r_2/r_{cut} = 0.6$. We call r_2 the cutoff radius of the DLL function.

In this paper we regard the gravitational field of the Sun as an external potential. This treatment is okay for the study of planet formation process of earth-type planets, because planetesimals do not perturb the Sun strongly. The total mass of planetesimals is much smaller than the mass of the Sun and planetesimals are distributed almost uniformly around the Sun.

We integrate H_{Soft} using the leapfrog and the tree method with a constant timestep Δt . We integrate H_{Hard} using the fourth-order Hermite method with the block timestep. For the timestep criterion, we used a slightly modified version of the ‘‘standard’’ criterion (Makino & Aarseth 1992 and Aarseth 2003). The standard criterion is given by

$$\Delta t_i = \eta \sqrt{\frac{|a_i^2| |a_i^{(2)}| + |\dot{a}_i|^2}{|\dot{a}_i| |a_i^{(3)}| + |a_i^{(2)}|^2}}, \quad (35)$$

where η is the accuracy parameter. The new timestep criterion we used is given as

$$\Delta t_i = \eta \sqrt{\frac{\sqrt{a_i^2 + a_0^2} |a_i^{(2)}| + |\dot{a}_i|^2}{|\dot{a}_i| |a_i^{(3)}| + |a_i^{(2)}|^2}}, \quad (36)$$

$$a_0 = \alpha^2 \frac{Gm_i}{r_H^2}. \quad (37)$$

Here a_0 is a constant introduced to prevent the timestep from becoming unnecessarily small when $|a_i|$ is small, and α is a parameter which controls the size of the timestep. Here, a_i is the acceleration due to F_{Hard} , and $\dot{a}_i, a_i^{(2)}$ and $a_i^{(3)}$ are its first, second and third time derivatives,

respectively, and m_i is the mass of particle. With equation (35), the timestep becomes unnecessarily small if there is just one particle inside the radius r_{cut} of one particle and $r_{ij} \simeq r_{cut}$. To illustrate this problem, consider the case in which one particle moves away radially with a constant velocity v . High order derivatives of the force from this particle is given by

$$a = FK, \quad (38)$$

$$\dot{a} = (F'K + FK')v, \quad (39)$$

$$a^{(2)} = (F''K + 2F'K' + FK'')v^2, \quad (40)$$

$$a^{(3)} = (F'''K + 3F''K' + 3F'K'' + FK''')v^3 \quad (41)$$

for the equation (35), where F is the gravitational force from a particle and K is the changeover function and $F'(x) = dF/dx$. In the case of $r_{ij} \lesssim r_{cut}$, we can expand K around r_{cut} . Without the loss of generality, we can assume that $r_{cut} = 1$ and $dr/dt = v = 1$. Then we have

$$K = -Z^5 + O(Z^6), \quad (42)$$

$$K' = -5Z^4 + O(Z^5), \quad (43)$$

$$K'' = -20Z^3 + O(Z^4), \quad (44)$$

$$K''' = -60Z^2 + O(Z^3), \quad (45)$$

where $Z \equiv \left(\frac{r_{ij}-r_{cut}}{r_{cut}}\right)$. By substituting equations (43)-(45) into equations (39)-(41), and omitting time derivatives of gravitational force, we obtain

$$a = -Z^5F + O(Z^6), \quad (46)$$

$$\dot{a} = -5Z^4F + O(Z^5), \quad (47)$$

$$a^{(2)} = -20Z^3F + O(Z^4), \quad (48)$$

$$a^{(3)} = -60Z^2F + O(Z^3). \quad (49)$$

Because time derivatives of gravitational force are individual to Z . Equation (35) becomes

$$\Delta t = \eta \sqrt{\frac{45Z^8F^2 + O(Z^9)}{700Z^6F^2 + O(Z^7)}}, \quad (50)$$

$$= \eta Z \sqrt{\frac{9 + O(Z)}{140 + O(Z)}}, \quad (51)$$

$$= \eta Z(1260 + O(Z)). \quad (52)$$

Equation (52) shows that the timestep approaches to zero as r_{ij} approaches to r_{cut} . This behaviour is clearly undesirable, since there is no need to reduce the timestep for the neighbour force, when the neighbour force itself is small. The reason why criterion (35) gives zero stepsize is, as we can see from equations (47)-(49), $|a|$ approaches to zero faster than its high order derivatives. However, this is due to the cutoff by the changeover function, and the actual physical acceleration by the particle just inside radius r_{cut} is of the order $\frac{m_j}{r_{cut}^2}$. In order to avoid this unnecessarily small timestep, we introduce a_0 in equation (37). By doing so, we make

criterion (37) to give the timestep which is accurate relative to the absolute strength of the force itself, before the changeover function is applied. This timestep criterion does not use the gravitational force from the Sun. In other words, the timestep is determined purely by the forces from nearby particles. If we included the Solar gravity, the original criterion could lead to unnecessarily small timesteps, since the Solar gravity is much larger than the forces from neighbour particles.

Our scheme is summarized as follows:

1. Make a tree at time t and calculate accelerations due to H_{Soft} .
2. Give a velocity kick.
3. Integrate positions and velocities from t to $t + \Delta t$ using the Hermite scheme with the block timestep and H_{Hard} .
4. Go back to step 1.

When we integrate H_{Hard} , we use the list of neighbours for particles to save the calculation time. If we do not use the neighbour lists, we have to calculate forces from all particles and the calculation cost becomes $O(N^2)$. We construct the neighbour list of particle i by selecting particles within distance r_{nl} from particle i at time t . Here r_{nl} must be sufficiently larger than r_{cut} , so that particles outside the radius r_{nl} do not enter the sphere of radius r_{cut} during one timestep. In this paper, we use $r_{nl} \gtrsim r_{cut} + 3\Delta t\sigma$, where σ is the the velocity dispersion. In order to find neighbours fast, we use a uniform 2-D grid with the grid size smaller than r_{cut} . To summarize our neighbour finding way, we first assign all particles to cells. We then look over the neighbouring cells which are within r_{nl} from a particle. The particles in the neighbouring cells are its neighbours.

4. Accuracy and Performance

In this section, we present the result of test calculations for the accuracy and performance of our new algorithm. We adopted the distribution of planetesimals following the Hayashi model for test calculations. The surface density at 1 AU is 10 g/cm^2 . The unit mass, the gravitational constant G , and the unit length are normalized to one solar mass, one, and 1 AU respectively. For most of the tests, we use 10000 equal-mass particles distributed randomly between the radii of 0.9 and 1.0 AU. Their mass is $1.45 \times 10^{23} \text{ g}$ and their velocities follow the Rayleigh distribution with $\langle e \rangle = 5r_H, \langle i \rangle = 2.5r_H$, where $\langle e \rangle$ and $\langle i \rangle$ are the dispersions of the eccentricity and inclination. Initial radius of particles is 364 km, which corresponds to the density of 3 g/cm^3 . Physical collisions are handled under the assumption of perfect accretion. The radius of the collision product is determined to keep the density unchanged. Unless specified otherwise, all test calculations are for 10 orbital periods.

Figures 2 and 3 show the relative energy error of the system, $|E - E_0|/|E_0|$ where E_0 is the energy of the system at time 0, and the number of direct gravitational interactions per

one tree timestep per one particle, N_{direct} , as a function of the cutoff radius r_{cut} , for the case of the spline changeover function (eq. 33). The cutoff radius r_{cut} is normalized by the Hill radius r_H at 1 AU. In figure 2, we plot the largest energy error during the time integration for 10yr (10 periods). We use $\eta = 0.05$, timestep $\Delta t = 0.040 - 0.0050$ yr, and opening angle $\theta = 0.5$ and 0.1 . The relative energy error is practically independent of r_{cut} if $r_{cut}/r_H > 3$ and $\Delta t < 0.020$ yr. The number of mutual interactions is proportional to the square of the cutoff radius (figure 3). Since the scale height of the disk is about $5r_H$, it is in most cases smaller than r_{cut} . Therefore the number of particles is proportional to the square of radius. Figures 2 and 3 show that by using $r_{cut}/r_H \sim 3$, we can achieve high accuracy with very small value of N_{direct} . On the other hand, the increase in the calculation cost is pretty small even when we use very large r_{cut}/r_H such as 50, because the force calculation using the tree is more expensive. In the case of $\theta = 0.5$, the energy error is lower-bounded at 10^{-8} , while with $\theta = 0.1$, the error can be reduced to 10^{-10} . In this case, using $\Delta t = 0.040$ yr resulted in a rather large error as shown in figure 2. This behaviour can be understood by looking at the time evolution of the error. Figure 4 shows the time evolution of the error for $\Delta t = 0.040$ yr and 0.010 yr. The behaviour of the error shows quasi-periodic behaviour with a period ~ 1 yr for $\Delta t = 0.040$ yr. In figure 2, the relative energy error for $\Delta t = 0.040$ yr, $r_{cut}/r_H = 20$ is larger than that for $\Delta t = 0.040$ yr, $r_{cut}/r_H = 7$. This is because the random energy error from tree scheme with large timestep is dominant for $\Delta t = 0.040$ yr. Thus, this peculiar behaviour occurred.

Figures 5 and 6 show the energy error for the case of the DLL cutoff functions, with the inner radius $r_1/r_H = 1$ and 10 . We can see that the behaviour of the error is quite similar to that in the case of the spline cutoff, and independent of the choice of r_1 .

Figures 7 and 8 show the relative energy error and the number of interactions per one particle in the tree part as a function of the opening angle θ . In figure 7, the energy error shows the power-law dependence as $\propto \theta^{2.5}$ for the case of $\Delta t = 0.0050$ yr. On the other hand, for $\Delta t = 0.040$ yr, the error dose not go below 10^{-9} for small values of θ . This is because, for $\Delta t = 0.040$ yr, the truncation error of the integrator becomes larger than the error due to force approximation for $\theta = 0.1$. In figure 8, the number of interactions per one particle is about two orders of magnitudes smaller than that for direct calculation, for $\theta = 0.1$. In figure 8, we can see that the dependence of N_{int} to θ is rather weak. In the case of stellar systems, calculation cost is proportional to $\theta^{-2\sim-3}$ (Makino 1991). In our experiment the dependence is $\sim \theta^{-1}$. This is because the distribution of particles is a thin and narrow ring. Figure 9 shows the relative energy error as a function of opening angle for the case of the DLL function again, the behaviour of the error is similar to the case of spline function.

Figure 10 shows the relative energy error as a function of the size of timestep for H_{Soft} . In the case of $\theta = 0.1$ and $\Delta t < 0.010$ yr, the error is dominated by that from the tree approximation, and becomes independent of Δt . If we want to keep the error in 10yr (10 periods) to be less than 10^{-9} , a pair of $\theta \sim 0.2$ and $\Delta t \sim 0.02$ is probably a good choice. In realistic calculations

10^{-9} in 10 orbits is probably okay, though how small the error should be is a difficult question. At least, the error of order of 10^{-9} is smaller than that of energy change of planetesimals due to gas drag and collisional damping. We do not show the result for the DLL cutoff here. We calculated by using same parameters for the DLL cutoff and confirmed that the result is essentially the same as that for the spline cutoff in figure 10.

Figures 11 and 12 show the relative energy error and the calculation cost of neighbour force N_{direct} as functions of the accuracy parameter η . Other parameters are $\theta = 0.1, r_{cut}/r_H = 10$ and $\Delta t = 0.0050$ yr. Figure 11 shows that the energy error is practically independent of the choice of α . On the other hand, in figure 12, small α results in the increase of N_{direct} . In practice, a pair of $\eta = 0.1$ and $\alpha = 1$ seems to be a good choice.

Figure 13 shows the long-term variation of the relative energy error. The calculation is done with the opening angle $\theta = 0.5$, the cutoff radius $r_{cut}/r_H = 10$ and the timestep $\Delta t = 0.0050$ yr. In this case, the energy error reaches about 7.5×10^{-8} after the time integration for 10^4 yr (10^4 orbital periods), while it is 9.8×10^{-9} for 10 yr (10 periods). In other words, the energy error grows 10 times larger as the integration time becomes 1000 times longer. It shows that the growth of energy error is stochastic like a random walk. It means that the error is mainly caused by the force error of the tree scheme (Barnes & Hut 1989). The growth of energy error is, therefore, expected to be slow and the error is small enough even after long calculations.

Figure 14 shows the calculation time per one tree timestep as a function of the total number of particles in the system N . The calculation is done with the opening angle $\theta = 1$, the cutoff radius $r_{cut}/r_H = 5$ and the timestep $\Delta t = 0.0050$ yr. We used the Intel(R) Core(TM)2 Quad CPU Q6600(2.4GHz). It shows that the calculation time increases as $O(N \log N)$. Therefore, we reduce the calculation cost from $O(N^2)$ to $O(N \log N)$.

Figure 15 shows the number of tree interactions, N_{tree} per particle as a function of N . We can see that N_{tree} is roughly proportional to $O(\log N)$.

5. Summary and Discussion

We have developed a new hybrid N -body simulation algorithm for the simulation of collisional N -body systems. This new scheme is constructed by combining the tree and direct schemes using the hybrid integrator. The results of test simulations of evolution of a planetesimal system show that our new scheme PPPT can drastically reduce the calculation cost, to the level comparable to the cost of a tree scheme with constant timestep while keeping accuracy sufficient for realistic simulations.

In principle, our scheme can be used for collisional systems other than planetary systems, such as globular clusters or stars around a supermassive blackhole in the galactic center. We'll show the results of simulations of such systems using our scheme in future.

We are grateful to Tomoaki Ishiyama, Masaki Iwasawa, Michiko Fujii, Kuniaki Koike,

Keigo Nitadori and Yusuke Tsukamoto for fruitful discussions. This work was partially supported by the Research Fund for Students (2009) of the Department of Astronomical Science, the Graduate University for Advanced Studies, KAKENHI 21244020 and 21220001.

References

- Aarseth, S. J. 1963, MNRAS, 126, 223
- Aarseth, S. J. 2003, Gravitational N-Body Simulations: Tools and Algorithms (Cambridge Monographs on Mathematical Physics)
- Abe, H., Sakairi, N., Itatani, R., Okuda, H., 1986, Comput. Phys., 63, 247
- Bagla, J. S. 2002, JA&A, 23, 185
- Barnes, J., & Hut, P. 1986, Nature, 324, 446
- Barnes, J., & Hut, P. 1989, ApJS, 324, 446
- Brunini, A., & Viturro, H. R. 2003, MNRAS, 346, 924
- Brunini, A., Santamaría, P. J., Viturro, H. R., & Cionco, R. G. 2007, P&SS, 55, 2121
- Bulirsch, R., Stoer, J. 1964, Num. Math. 6, 413
- Calvo, M. P., & Sanz-Serna, J. M. 1993, SIAM J. Sci. Comput., 14, 4, 936
- Chambers, J. E. 1999, MNRAS, 304, 793
- Dubinski, J., Kim, J., Park, C., & Humble, R. 2004, New Astron., 9, 111
- Duncan, M. J., Levison, H. F., & Lee, M. H. 1998, AJ, 116, 2067
- Fehlberg, E. 1968, NASA TR R 287
- Fujii, M., Iwasawa, M., Funato, Y., & Makino, J. 2007, PASJ, 59, 1095
- Hockney, R.W., & Eastwood, J.W. 1981, Computer Simulation Using Particles (New York: McGraw-Hill)
- Ishiyama, T., Fukushige, T., & Makino, J. 2009, PASJ, 61, 1319
- Kinoshita, H., Yoshida, H., & Nakai, H. 1991, Celest. Mech. Dyn. Astron., 50, 59
- Levison, H. F., & Duncan, M. J. 2000, AJ, 120, 2117
- Makino, J., & Aarseth, S. J. 1992, PASJ, 44, 141
- Makino, J. 1991, PASJ, 43, 859
- McMillan, S. L. W., & Aarseth, S. J. 1993, ApJ, 414, 200
- Moore, A. J., Quillen, A. C., & Edgar, R. G. 2008, arXiv0809.2855
- Skeel, R. D. & Biesiadecki, J. J. 1994, Ann. Numer. Math, 1, 191
- Skeel, R. D. & Gear, C. F. 1992, Physica, D60, 311
- Springel, V. 2005, MNRAS, 364, 1105
- Stoer, J., & Bulirsch, R. 1980, Introduction to Numerical Analysis (Springer Verlag, New York)
- Wisdom, J., & Holman, M. 1991, AJ, 102, 1528
- Xu, G. 1995, ApJS, 98, 355
- Yoshikawa, K., & Fukushige, T. 2005, PASJ, 57, 849

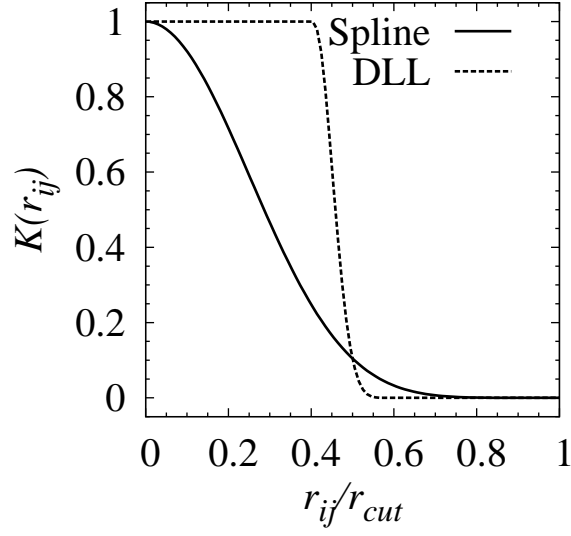


Fig. 1. The changeover functions. The horizontal axis is the distance between i and j particles normalized by the cutoff radius, and $K(r_{ij})$ is the changeover function. The solid and dashed curve, show the fourth order spline function and the DLL function. This function uses $r_1/r_{cut} = 0.4$ and $r_2/r_{cut} = 0.6$.

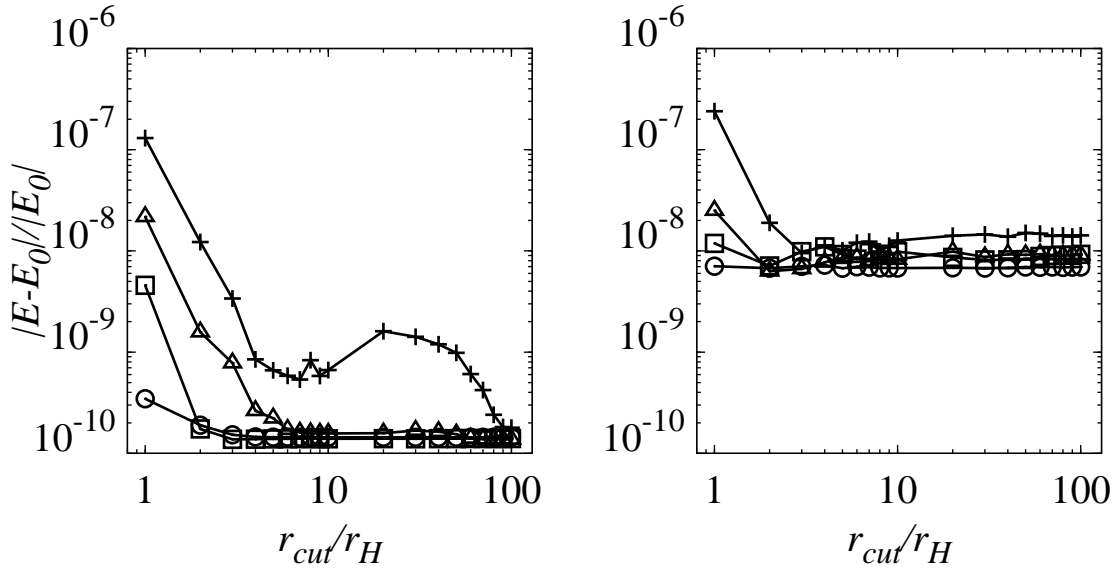


Fig. 2. The energy error plotted against the cutoff radius. Crosses, triangles, squares and circles show the results with $\Delta t = 0.04, 0.02, 0.01$ and 0.005 yr, respectively. The left and right panels show the results with $\theta = 0.1$ and 0.5 , respectively.

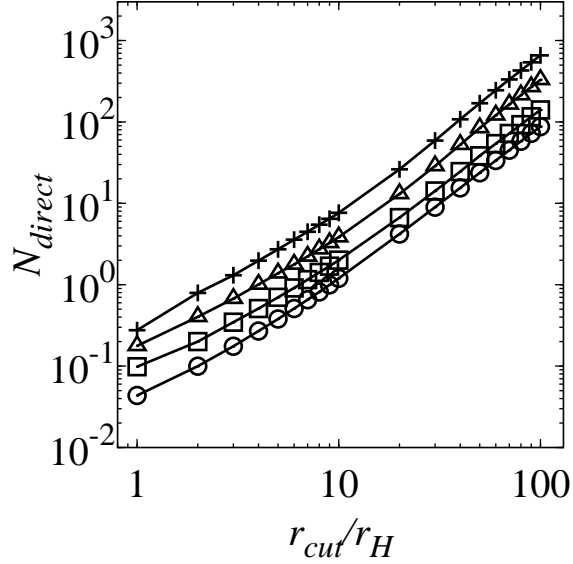


Fig. 3. The number of direct gravitational interactions per one tree timestep per one particle with the spline function plotted against the cutoff radius. Crosses, triangles, squares and circles show the results with $\theta = 0.1, \Delta t = 0.04, 0.02, 0.01$ and 0.005 yr, respectively.

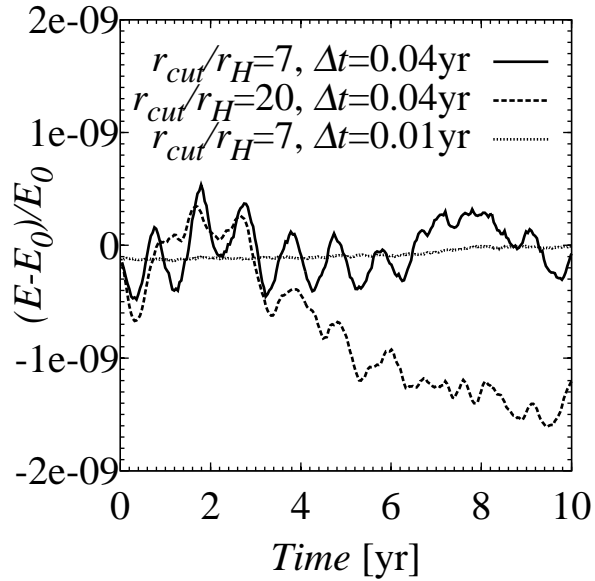


Fig. 4. The relative energy error of the system with the spline function plotted against the calculation time. The solid curve shows the result with $\Delta t = 0.04$ yr, $r_{cut}/r_H = 7$ and $\theta = 0.1$. The dashed curve shows the result with $\Delta t = 0.04$ yr, $r_{cut}/r_H = 20$ and $\theta = 0.1$. The dotted curve shows the result with $\Delta t = 0.01$ yr, $r_{cut}/r_H = 7$ and $\theta = 0.1$.

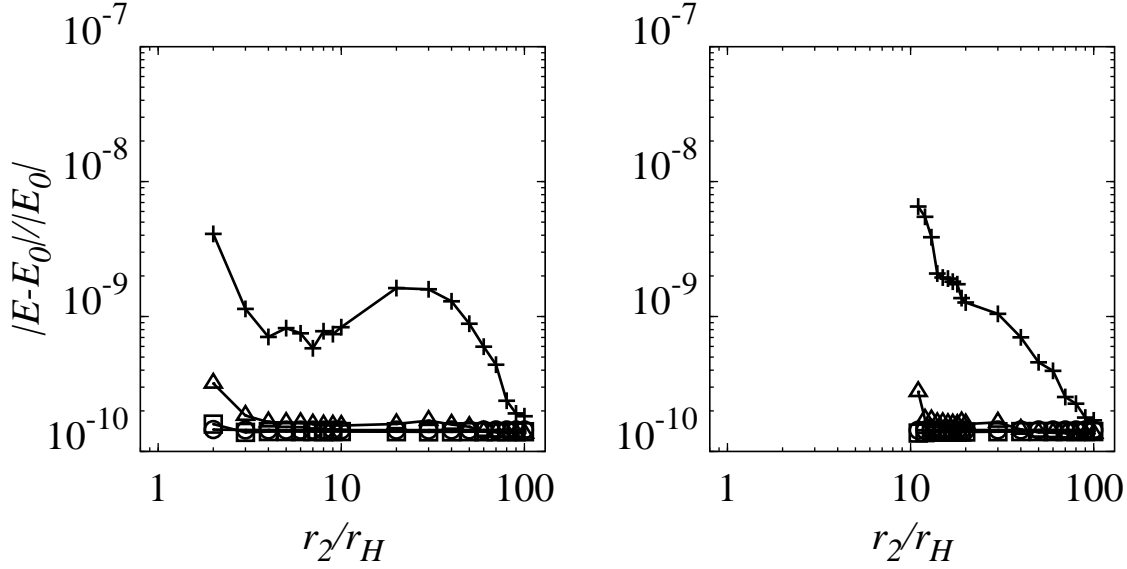


Fig. 5. The relative energy error of the system with the DLL function plotted against the r_2 cutoff radius. Crosses, triangles, squares and circles show the results with $\Delta t = 0.04, 0.02, 0.01$ and 0.005 yr, respectively. The left and right panels show the results with $r_1/r_H = 1, r_2/r_H = 2 - 100, \theta = 0.1$ and $10, 11 - 100, 0.1$, respectively.

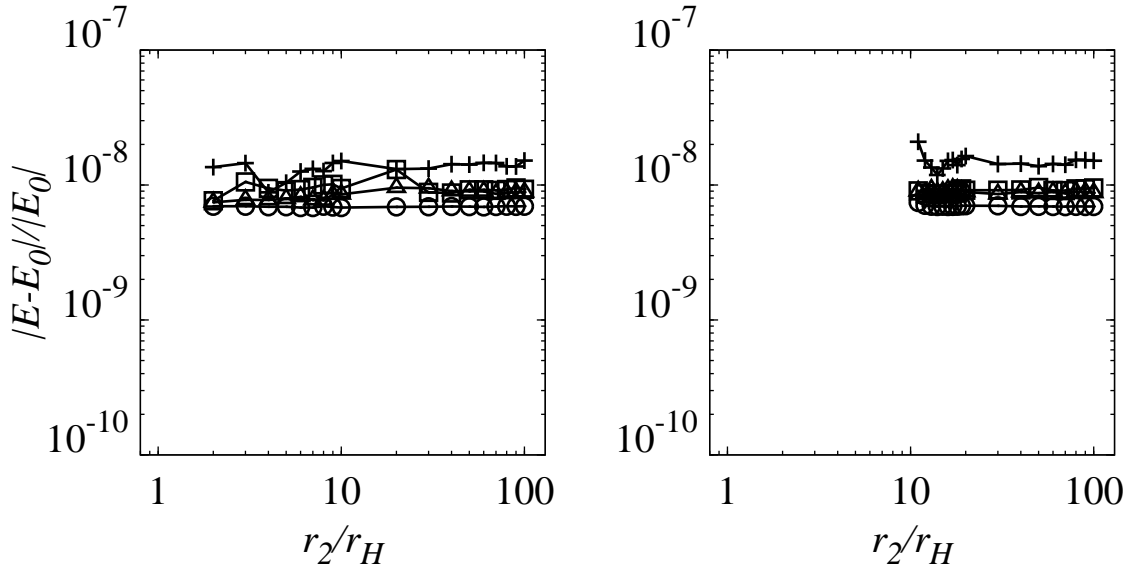


Fig. 6. The relative energy error of the system with the DLL function plotted against the r_2 cutoff radius. Crosses, triangles, squares and circles show the results with $\Delta t = 0.04, 0.02, 0.01$ and 0.005 yr, respectively. The left and right panels show the results with $r_1/r_H = 1, r_2/r_H = 2 - 100, \theta = 0.5$ and $10, 11 - 100, 0.5$, respectively.

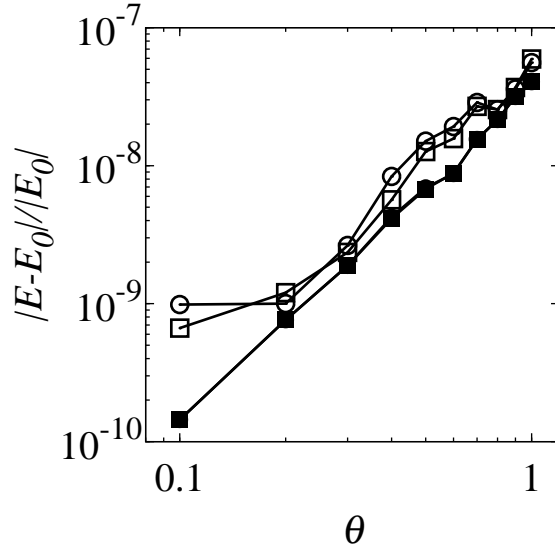


Fig. 7. The relative energy error of the system with the spline function plotted against the opening angle θ . Open squares, open circles, filled squares and filled circles show the results with $r_{cut}/r_H = 10$ and $\Delta t = 0.04$ yr, $r_{cut}/r_H = 50$ and $\Delta t = 0.04$ yr, $r_{cut}/r_H = 10$ and $\Delta t = 0.005$ yr and $r_{cut}/r_H = 50$ and $\Delta t = 0.005$ yr, respectively.

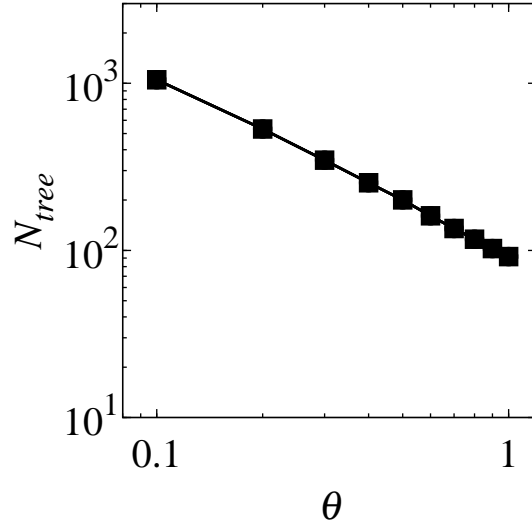


Fig. 8. The number of tree gravitational interactions per one tree timestep per one particle with the spline function plotted against the opening angle θ . Open squares, open circles, filled squares and filled circles show the results with $r_{cut}/r_H = 10$ and $\Delta t = 0.04$ yr, $r_{cut}/r_H = 50$ and $\Delta t = 0.04$ yr, $r_{cut}/r_H = 10$ and $\Delta t = 0.005$ yr and $r_{cut}/r_H = 50$ and $\Delta t = 0.005$ yr, respectively. The four results are practically indistinguishable.

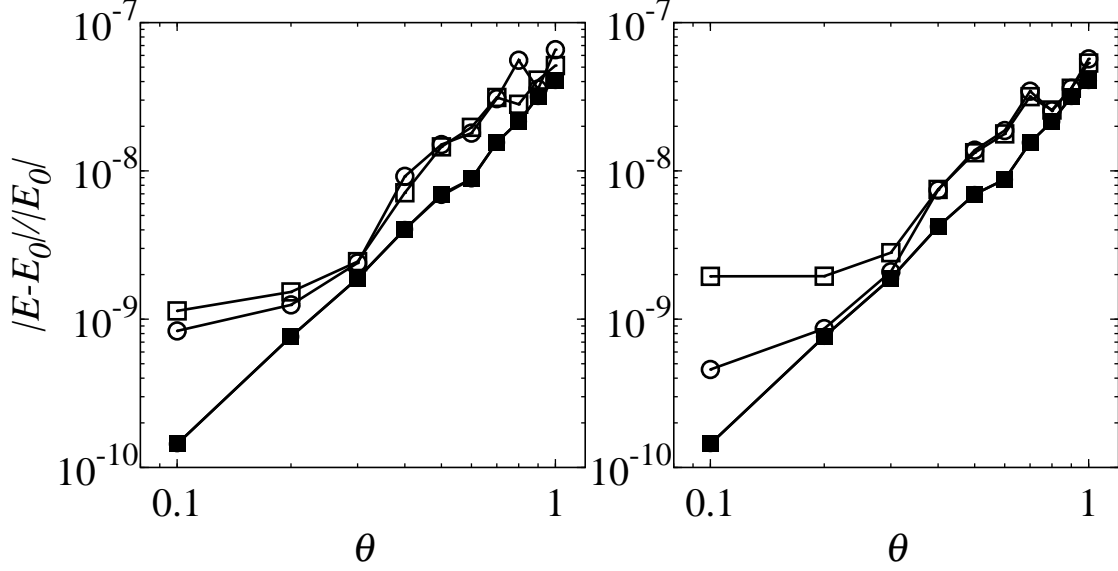


Fig. 9. The relative energy error of the system with the DLL function plotted against the opening angle θ . The left panel shows the results with $r_1/r_H = 1$ and open squares, open circles, filled squares and filled circles show the results with $r_2/r_H = 3$ and $\Delta t = 0.04$ yr, $r_2/r_H = 10$ and $\Delta t = 0.04$ yr, $r_2/r_H = 3$ and $\Delta t = 0.005$ yr and $r_2/r_H = 10$ and $\Delta t = 0.005$ yr, respectively. The right panel shows the results with $r_1/r_H = 10$ and open squares, open circles, filled squares and filled circles show the results with $r_2/r_H = 15$ and $\Delta t = 0.04$ yr, $r_2/r_H = 50$ and $\Delta t = 0.04$ yr, $r_2/r_H = 15$ and $\Delta t = 0.005$ yr and $r_2/r_H = 50$ and $\Delta t = 0.005$ yr, respectively.

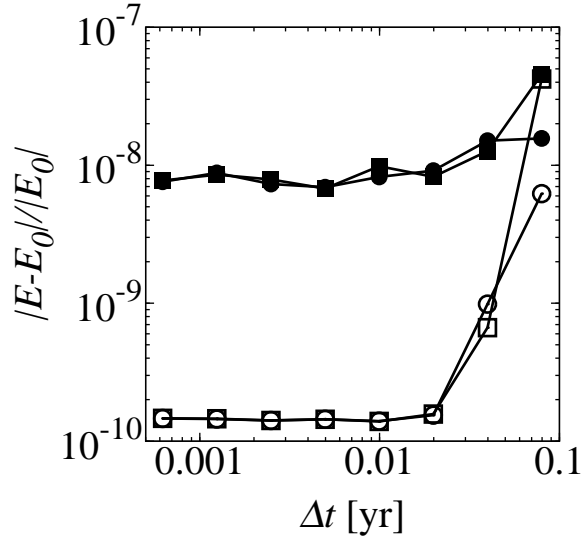


Fig. 10. The relative energy error of the system with the spline function plotted against the tree timestep. Open squares, open circles, filled squares and filled circles show the results with $\theta = 0.1$ and $r_{cut}/r_H = 10$, $\theta = 0.1$ and $r_{cut}/r_H = 50$, $\theta = 0.5$ and $r_{cut}/r_H = 10$, $\theta = 0.5$ and $r_{cut}/r_H = 50$, respectively.

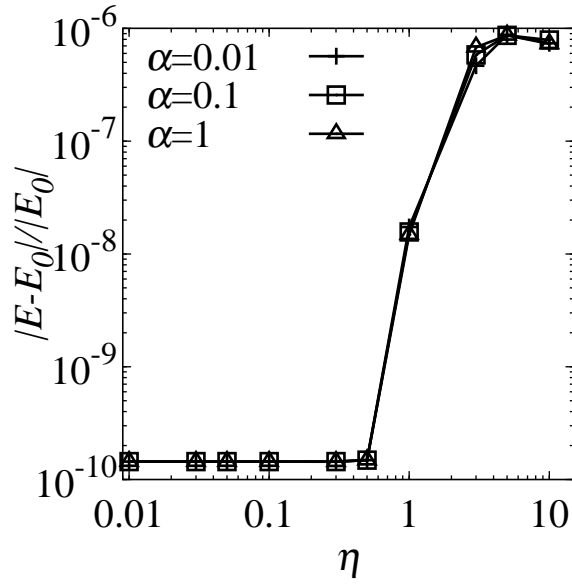


Fig. 11. The relative energy error of the system plotted against the timestep accuracy parameter η . Crosses, squares and triangles show the results with $\alpha = 1, 0.1$ and 0.01 , respectively.

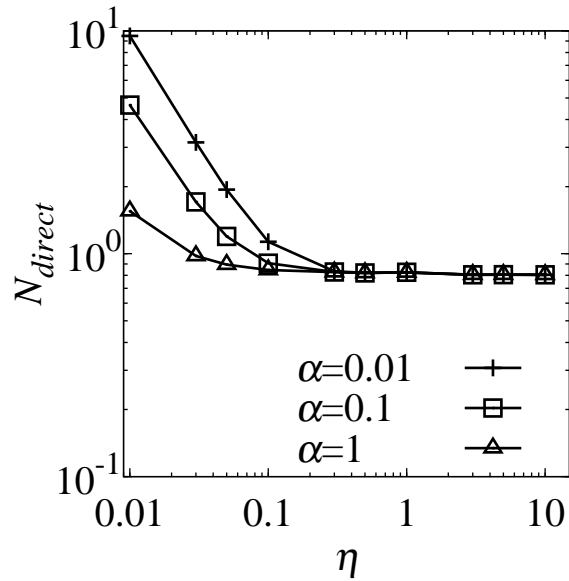


Fig. 12. The number of direct gravitational interactions per one tree timestep per one particle with the spline function plotted against the timestep accuracy parameter η . Crosses, squares and triangles show the results with $\alpha = 1, 0.1$ and 0.01 , respectively.

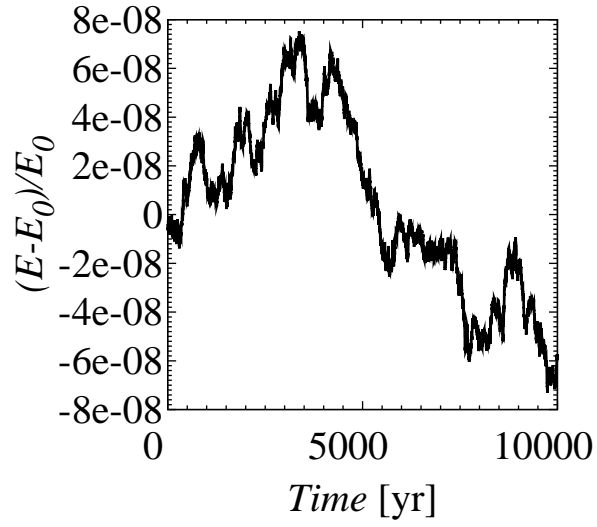


Fig. 13. Energy error of the system plotted against a function of time.

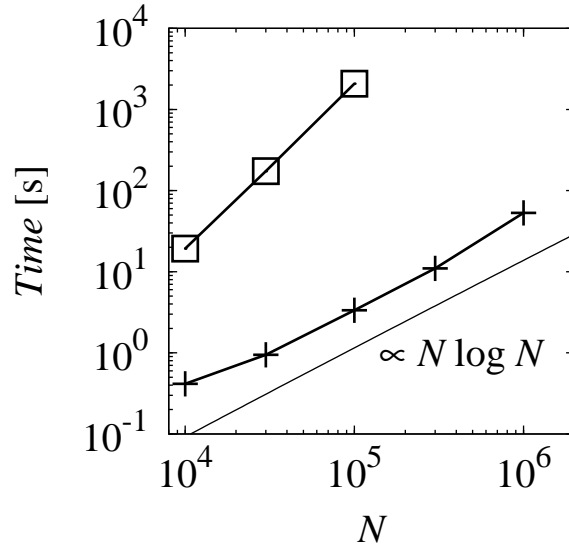


Fig. 14. Calculation time per 0.0050 yr plotted against a function of number of particles. Crosses and squares show the results of PPPT and fourth-order Hermite scheme, respectively.

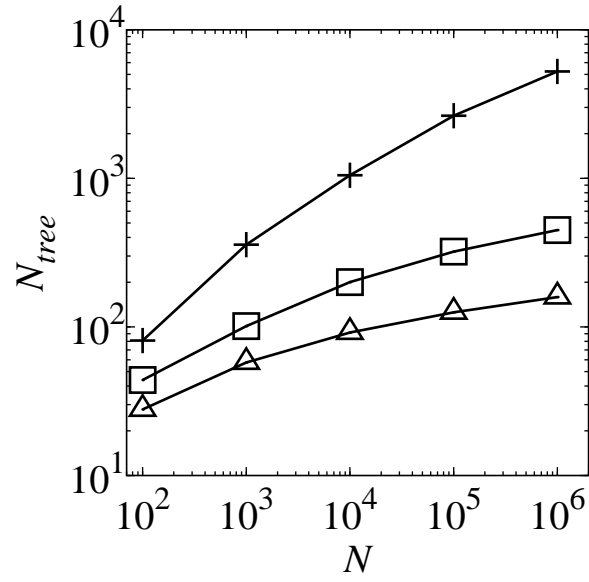


Fig. 15. The number of tree gravitational interactions per one tree timestep per one particle with the spline function plotted against a function of number of particles. Crosses, open squares and open triangles show the results with $\theta = 0.1, 0.5$ and 1 , respectively.